Marine Geology 477 (2024) 107408

Contents lists available at ScienceDirect

Marine Geology

journal homepage: www.elsevier.com/locate/margo

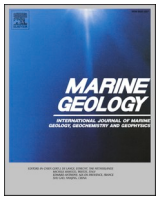

Research Article

Hawaiian legends of coastal devastation and paleotsunami reconstruction, Nu'u, Kaupō, Maui, Hawai'i

Scott Fisher [a,c,*], James Goff [b,c], Andrew Cundy [c], David Sear [d], James Terry [e], Randall J. LeVeque [f], Loyce M. Adams [f], Diana Sahy [g]

[a] Hawai'i Land Trust, PO Box 965, Wailuku, Hawai'i 96793, USA
[b] Earth and Sustainability Science Research Centre (ESSRC), School of Biological, Earth and Environmental Sciences, UNSW Sydney, Kensington, NSW 2052, Australia
[c] School of Ocean and Earth Science, University of Southampton, National Oceanography Centre (Southampton), Southampton, UK
[d] School of Geography & Environmental Science, University of Southampton, Highfield, Southampton, UK
[e] College of Natural and Health Sciences, Zayed University, Dubai, United Arab Emirates
[f] Department of Applied Mathematics, University of Washington, Seattle, WA 98195, USA
[g] National Isotope Laboratory, British Geological Survey, Keyworth, NG12, 5GG, UK

ARTICLE INFO

Editor: Edward Anthony

Keywords:
Oral traditions
Submarine landslides
Tsunamis
Wedge clasts
Minimum flow velocities
Tsunami modeling

ABSTRACT

In Hawai'i, tsunamis are often described in orally transmitted legends (*mo'olelo*). This study examines sedimentary evidence of a possible local submarine landslide-generated tsunami, described in a legend from the south east coast of Maui which originated between the 15th Century CE and the first arrival of Europeans in 1778 CE. Physical evidence for a tsunami, found at the Nu'u Refuge, Maui, is primarily comprised of an extensive coral clast deposit (found 8.5 m above msl and 251 m inland from the shoreline) together with waterworn cobbles which form fracture-embedded wedge clasts in a local basalt escarpment (at up to 8 m above msl). U/Th dating of the coral clasts gives a maximum tsunami deposit age of 1671 CE for the event that may have inspired the local *mo'olelo*. This depositional sequence is used to characterize the nature of the assumed tsunami in terms of inundation distance, maximum wave runup and minimum flow velocities. A numerical model developed using GeoClaw matches well with the physical evidence. The data and modeling presented here suggest that locally-generated tsunamis from submarine landslides warrant further research attention as sources of destructive high energy marine inundation events.

1. Introduction

In the 21st century tsunamis have claimed the lives of nearly 250,000 individuals worldwide, making them one of the most deadly and destructive natural disasters, impacting both economic development and the integrity of coastal ecosystems (Tanaka et al., 2009; Reid and Mooney, 2023). In areas prone to tsunamis, their signature on the landscape has been recognized to last for centuries or longer, and they are known to transport large objects substantial distances inland, including ships, cetaceans and large coral boulders (Goff and Dudley, 2021; Goff and Chagué-Goff, 2009). Tsunamis have also been recognized as agents shaping both cultural and settlement patterns in the eastern Mediterranean, the United Kingdom, Melanesia and Polynesia, among others (McClintock et al., 2023; Shtienberg et al., 2020; Smith et al., 2004; Goff and McFadgen, 2001; Cain et al., 2007).

In regions with relatively short (written) historical periods, such as North America, Australasia and Oceania, paleotsunami research often includes the study of pre-historic orally transmitted accounts. These accounts can be used to provide a deeper understanding of both the destructive capacity of these events and vulnerabilities to future tsunami impact (Dawson and Stewart, 2007a). Accurate characterization of tsunami frequency and intensity remains a key component in designing strategies to mitigate their destructive capacity (Goff, 2011).

On average, Hawai'i experiences destructive tsunamis about once every 11 years, making it among the most tsunami-prone locations in the world (Fisher et al., 2023). Across the archipelago, historic tsunamis, particularly the 1946 Aleutian Islands and 1960 Valdivia, Chile events, have claimed the lives of over 200 individuals making them the most

* Corresponding author at: Hawai'i Land Trust, PO Box 965, Wailuku, Hawai'i 96793, USA.
E-mail addresses: Scott@hilt.org (S. Fisher), j.goff@unsw.edu.au, jg4e18@soton.ac.uk (J. Goff), A.Cundy@soton.ac.uk (A. Cundy), D.Sear@soton.ac.uk (D. Sear), James.Terry@zu.ac.ae (J. Terry), rjl@uw.edu (R.J. LeVeque), lma3@uw.edu (L.M. Adams).

https://doi.org/10.1016/j.margeo.2024.107408
Received 10 June 2024; Received in revised form 19 September 2024; Accepted 27 September 2024
Available online 4 October 2024

deadly natural disaster in Hawai'i (Fisher et al., 2023). In prehistoric Hawai'i, legends of tsunamis are often incorporated into the corpus of orally transmitted stories, or *mo'olelo,* in order to both convey important cultural values and to identify threats to the local community (Brown, 2022; Beckwith, 1982).

The aim of this study lies in establishing the paleotsunami history of the 32-ha Nu'u Refuge on Maui's south east coast. We do so by hypothesizing that a traditional *mo'olelo* from south east Maui describes a locally-generated tsunami which impacted the Nu'u Refuge sometime between 1671 CE and 1778 CE. In doing so we set out to accomplish three tasks related to developing this hypothesis. First, we review the *mo'olelo* recorded from Maui's south east coast that indicates a high energy marine inundation (HEMI) event during prehistoric times. Second, through field data collected from Kaupō district on Maui's south east coast at Nu'u Bay (Fig. 1) we characterize the event most likely referred to in the *mo'olelo* in terms of run-up height, inundation distance,

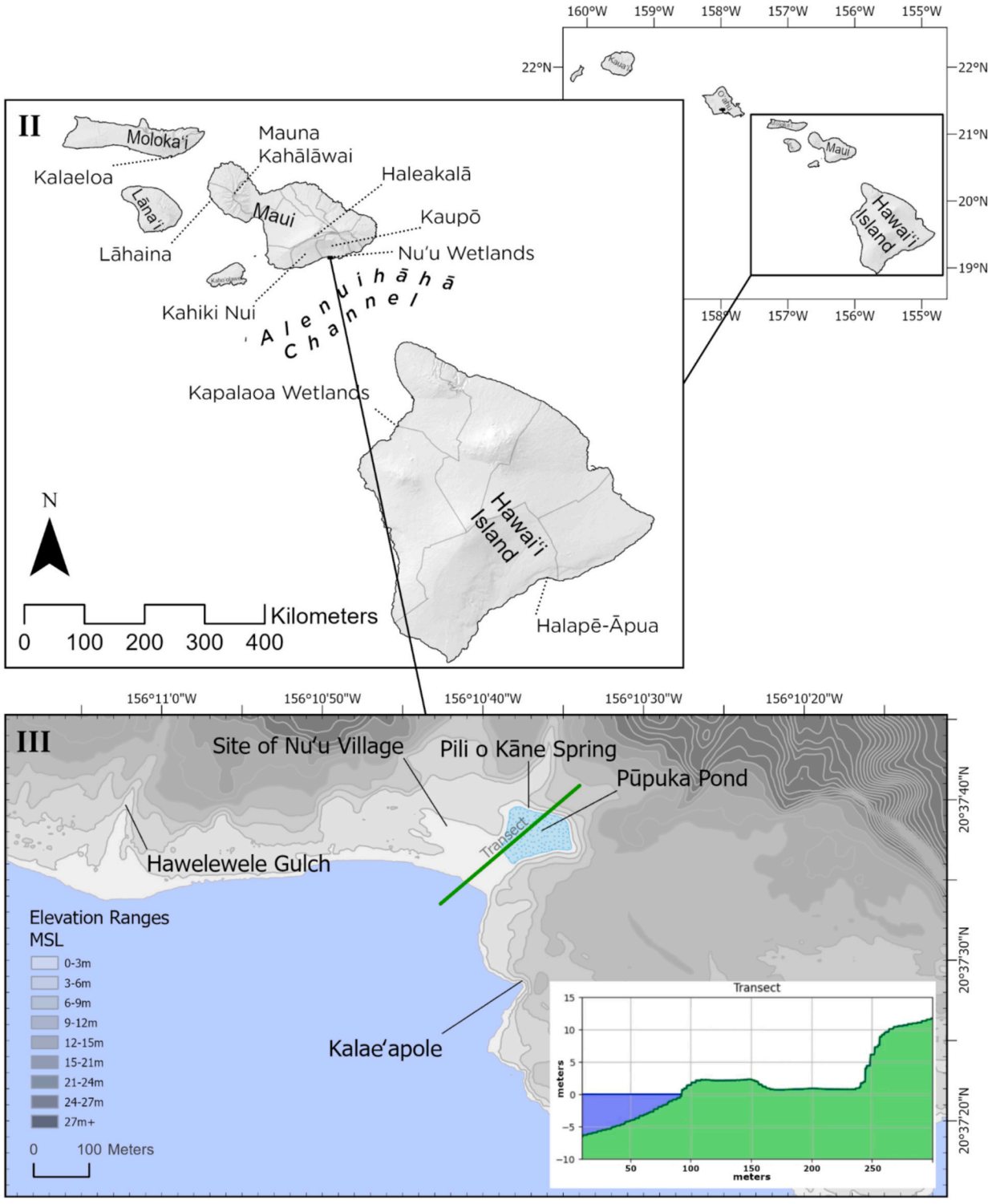

Fig. 1. Map of the Hawaiian Islands and the Nu'u Refuge with sites mentioned in the text. The highest point on the refuge, to the north east of Pūpuka pond, is 11.8 m above sea level.

flow velocity and timing. We do this by examining three widely accepted proxies for flood and tsunami inundation. These include the use of small coral clasts to date the event and determine the approximate limit of inland inundation; utilizing waterworn cobbles and coral clasts wedged into a coastal escarpment (wedge clasts) to determine maximum wave heights; and using coral boulders surrounding Pūpuka pond in the Nu'u Refuge to calculate minimum flow velocities (Figs. 2, 3). Third, by using the proxy data acquired we propose a hypothetical tsunami model that could have produced results similar to those observed in the field.

Tsunami impact modeling illustrates the intensity of tsunami inundation, particularly for well-documented historically recorded events with run-up data collected soon after the event.

Tsunami modeling is widely used to determine unmeasurable characteristics of the event and provide valuable evidence for their power and dynamics, usually in the aftermath of an event. Their application to paleotsunami is helpful in determining the frequency and magnitude of such events allowing more recent tsunamis to be put into a longer term context (Bosserelle et al., 2020).

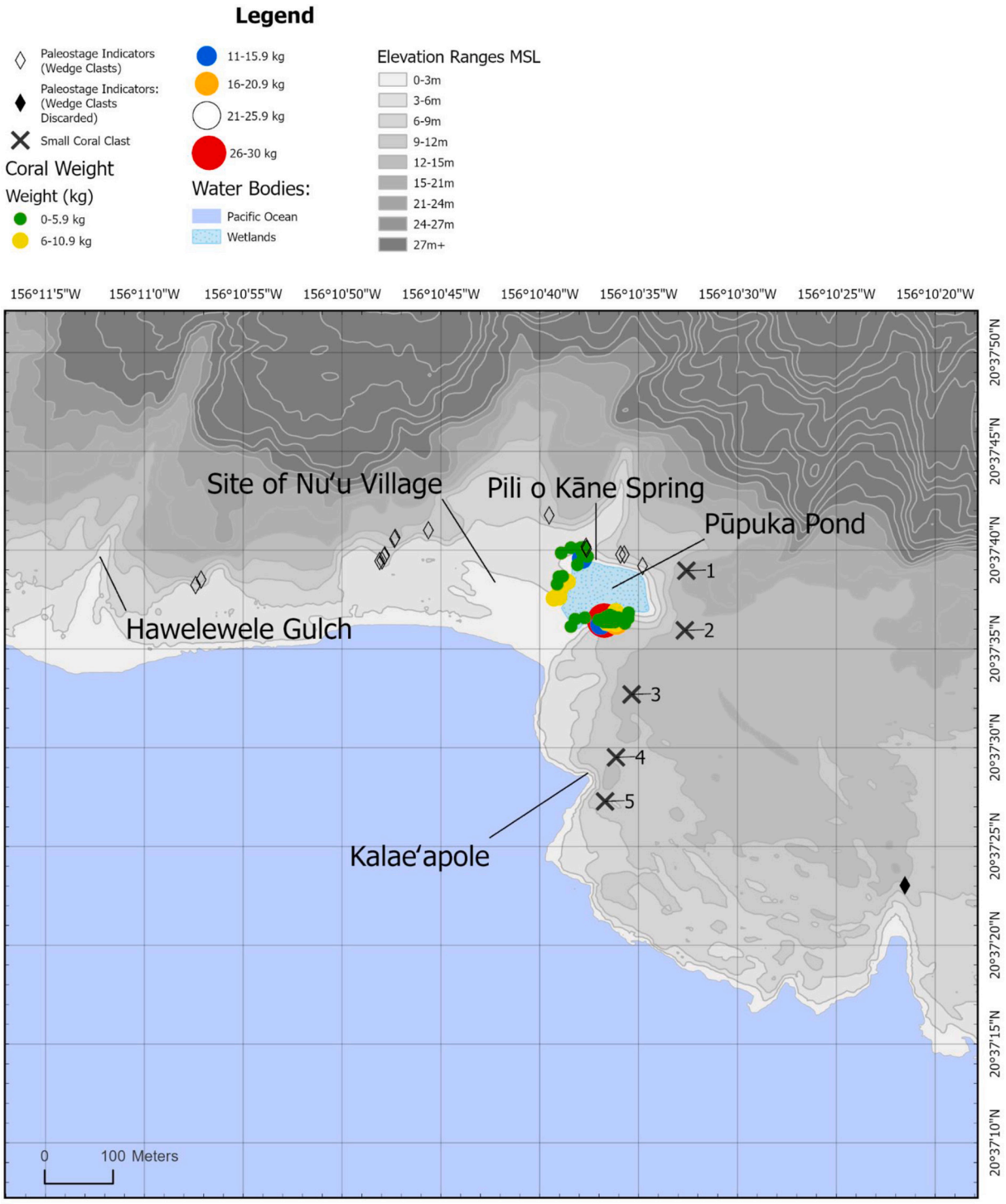

Fig. 2. Coral boulders (colour coded by weight), paleostage indicators and small coral clasts around Pūpuka pond.

Fig. 3. Paleostage indicators: wedge clast #11 found at Pūpuka pond at an elevation of 3.75 m above msl. (a) Circle includes four wedge clasts; (b) Up close view of the same wedge clasts.

2. Study area

2.1. The Island of Maui and Nu'u, Kaupō

Maui is the second largest island in the Hawaiian archipelago with an area of 1883 km^2 (Juvik and Juvik, 1999). It lies toward the south eastern end of the Hawaiian archipelago, and consists of two shield volcanoes, the older Mauna Kahalawai to the west and Haleakalā to the east (Fig. 1). The study area, Nuʻu, in the Kaupō district, is located on the southern slopes of Haleakalā, and is known as a traditional land section, or *ahupuaʻa*, within the district of Kaupō (Fig. 1).

Evidence of permanent human habitation in the Kaupō district begins in the 15th century with the early Hawaiian community practicing both fishing and sweet potato farming (Baer, 2015; Kirch et al., 2009). In the 19th century, cattle ranching and salt production dominated the economic life of Nuʻu (Maunupau, 1998; Walmisley, 2021). A map produced in 1882 CE indicates a total of 8 homes in Nuʻu village adjacent to the pond, with an additional 16 structures in the area.

On April 1st, 1946 a tsunami originating in the Aleutian Islands generated waves at Nuʻu exceeding 3 m, damaging several homes in the village and precipitating its abandonment (Loomis, 1976). In 2011, after approximately 150 years of cattle ranching, the Hawaiʻi Land Trust, a local conservation organization, purchased the 32 ha Nuʻu Refuge with the intention of restoring the degraded ecology around Pūpuka pond (discussed below) and preserving and protecting significant archaeological sites.

The Nuʻu Refuge consists of three geological and ecological units, including a coastal plain, a palustrine discharge wetland and a geologically young lava peninsula. The first unit consists of 9.5 ha of coastal plains composed mainly of basalt sand, gravel, cobbles and boulders near the coast, and mixed colluvial soil and basalt cobbles and boulders further inland. The cobble and boulder fore-bench along the coast reaches approximately 2 m above msl with the coastal plain varying in width between 100 and 300 m, ending at a columnar basalt shelf approximately 6–9 m above msl (3–5 m above ground level) at its eastern end. A second unit consists of a 2.5-ha palustrine discharge wetland, known as the Pūpuka pond, lying approximately 1–2 m above msl, and surrounded by a 9 m cliff on three sides. The third unit includes a 20 ha peninsula of *aʻa* lava known as Kalaeʻapole, the result of a lava flow occurring approximately 1160 +/− 50 BP (Sherrod et al., 2006). Kalaeʻapole's highest point, and the highest point on the Nuʻu Refuge, lies inland near a state highway at approximately 23 m above msl (Fig. 1).

2.2. Pūpuka Pond

Pūpuka pond has been recognized as ecologically significant, serving as both high quality habitat and a transit point for endangered Hawaiian waterbirds for their travel across the 51 km ʻAlenuihāhā Channel between Maui and Hawaiʻi Island (Bruland and MacKenzie, 2010, Fig. 1). Considering its critical habitat, the Hawai'i Land Trust is committed to mitigating the deposition of sedimentary material into the Pūpuka wetlands during HEMI events.

3. Materials and methods

3.1. Legends of catastrophic saltwater inundation events at Nu'u and across Hawai'i

Orally transmitted legends have become an important tool to identify and characterize catastrophic inundation events, including tsunamis (Lavigne et al., 2021; Goff and Nunn, 2016; Clark and Reepmeyer, 2014). For this study we conducted a review of orally transmitted legends from the region, in both English and Hawaiian language newspapers and other published material for references to HEMI events (Brown, 2022; Beckwith, 1982; Maunupau, 1998; Kalaowali, 1891). This survey included references to any marine inundation across the archipelago, with special attention paid to Maui's south east coast. All translations were made by the lead author.

3.2. Wrack line distribution of small coral clasts and chronological controls

Wrack lines mark the terminal (or near terminal) extent of tsunami inundation. This line was mapped on Kalaeʻapole using a Sparkfun RTK Global Navigation Satellite System (GNSS) (accuracy +/− 1.4 cm) following an easily distinguishable series of small coral clasts (Fig. 2). The data were processed and mapped in Arc-GIS 10.8. Five coral clasts were collected for U—Th dating (sup. Table s1).

Collection criteria of coral clasts for dating included both angularity of the clasts and distance from recognized archaeological sites and trails. Selection of angularity ensured brevity between breakage and deposition. In Hawai'i such coral clasts are known to mark trails on lava fields and are often associated with ritual and other archaeological sites (Gregg et al., 2015). In order to avoid anthropogenically deposited coral, fragments closer than 50 m from recognizable archaeological sites and trails were avoided, and, where possible, clasts were selected that underlay other basalt rocks (i.e. those obviously not deposited as trail markers). U—Th dates of these coral clasts were determined by the British Geological Survey, National Environmental Isotope Facility following the procedures of Crémière et al. (2016),

3.3. Paleostage indicators: wedge clasts

Paleostage indicators (PSI) include a variety of material from which researchers can infer flood stages or, in the case of tsunamis, maximum runup heights (O'Connor and Baker, 1992). Typically, PSI include eroded basalt benches, geomorphic surfaces such as terraces or floodplains, ice-rafted erratics, and exotic rock types (O'Connor and Baker, 1992; Jarrett and England Jr., 2002). A total of 130 vertical fractures along a 1.25 km length of coast were inspected, with 16 fractures containing one or more waterworn cobbles or coral clasts (Figs. 2 and 3, sup. Table s2). Wedge clasts were mapped using GNSS and data collected on elevation above sea level and distance from the ocean. Additional data included type (basalt waterworn cobble or coral clast), orientation in degrees and measurements of length (x-axis average) width (y-axis average) and height (z- axis average), where possible (sup. Table s2). Wedge clast data were processed and mapped in Arc-GIS 10.8.

While we cannot definitively discount anthropogenic or other natural means of wedge clast emplacement, we adhered to a strict protocol to minimize this possibility. For inclusion in this study wedge clasts had to meet three criteria. First, only waterworn basalt cobbles or coral were counted (i.e. those deriving from, or shaped by, the ocean). Second, only those clasts embedded in the vertical crevices which could not be easily extracted by hand were included. Finally, clasts which could have possibly fallen from above (i.e. crevices wider at the top) were excluded. Additionally, where clusters of wedge clasts were found, measurements included only the highest clast (sup. Table s2).

3.4. Coral boulder deposits

Post-tsunami surveys of coral boulders have been utilized to characterize inland inundation distances and minimum flow velocities on Ishigaki Island, Japan; Tongatapu, Tonga; Savaii and Upolu, Samoa; Oʻahu, Hawai'i; Sumatra, Indonesia; and numerous other locations (Etienne et al., 2011, Goto et al., 2010, Frohlich et al., 2009, Keating et al., 2004).

Coral deposits of clasts over 20 cm in length ($n = 63$) were sampled around Pūpuka pond for weight (kg), length (a-axis), width (b-axis) and height (c-axis), orientation (degrees), slope angle above mean tide level and elevation (m above sea level; Fig. 2, sup. Tables S3 and S4). Coral boulders found within 30 m of identifiable archaeological sites were not included in this study. Coral boulder distribution patterns were mapped using Arc-GIS (Fig. 2).

Clast volume (V, m^3) and mass (M, kg) were calculated from clast dimensions. For irregularly-shaped clasts with eroded edges and corners, volumes are typically overestimated by simply multiplying the axes (a × b × c). A better approach is to calculate clast volume as the best-fitting ellipsoid:

$$V = \frac{4}{3}\pi\left(\frac{a}{2}.\frac{b}{2}.\frac{c}{2}\right)$$

Clast mass (kg) was subsequently estimated from ρ × V, where ρ is the density of coral limestone (1.8 t/m^3).

Characteristics of shoreward minimum flow velocities (MFVs) generated by (paleo)tsunamis, presumed as responsible for the landward transport of coral clasts, can be calculated by applying hydrodynamic flow-transport (HFT) equations (Fig. 4). MFVs were thus calculated using clast dimensions and beach slope, under a variety of assumed modes of clast transport, including sliding, overturning and lifting. The following formulas and coefficients were used, based upon the widely-adopted HFT equations of Nandasena et al. (2011), modified by Terry and Malik (2020) for high-energy flows containing elevated sediment concentrations:

$$u^2 \geq \frac{2\left(\frac{\rho_b}{C_\rho \cdot \rho_w} - 1\right) gc\ (\mu_s cos\,\theta + sin\,\theta\ )}{C_d\left(\frac{c}{b}\right) + \mu_s C_l}$$

Eq.1 for clast transport by sliding

$$u^2 \geq \frac{2\left(\frac{\rho_b}{C_\rho \cdot \rho_w} - 1\right) gc\ \left(cos\,\theta + sin\left(\frac{c}{b}\right) sin\,\theta\ \right)}{C_d\left(\frac{c^2}{b^2}\right) + C_l}$$

Eq.2 for clast transport by overturning

$$u^2 \geq \frac{2\left(\frac{\rho_b}{C_\rho \cdot \rho_w} - 1\right) gc\ cos\theta}{C_l}$$

Eq.3 for clast transport by lifting.where u is flow velocity (m/s) and all other parameters and coefficients are as given in Table 1.

Table 1. Parameters used in hydrodynamic flow transport equations. C_ρ is a multiplier for clear-seawater density, for conditions of elevated sediment content (as suspension and saltation load) during a tsunami. Here we adopt a conservative value of 5 % sediment concentration of basaltic (volcanic) sands and pebbles in the tsunami flow. See Terry and Malik (2020) for further details.

3.5. Tsunami impact modeling

Models of the 1946 Aleutian Islands and 1960 Valdivia, Chile events, the two most powerful 20th century tsunamis, failed to produce wave velocities or inundation distances sufficient to either transport coral boulders into Pūpuka pond or more generally to match material found in

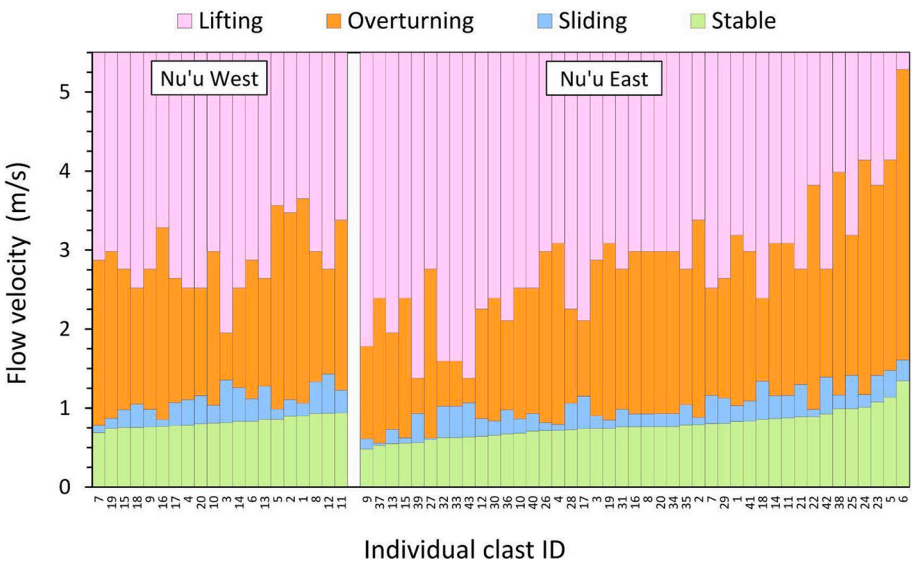

Fig. 4. Minimum flow velocities under various transport conditions for numbered coral clasts.

Table 1
Parameters used in hydrodynamic flow transport equations.

Symbol	Parameter
a	clast a-axis (long axis, m)
b	clast b-axis (intermediate axis, m)
c	clast c-axis (short axis, m)
C_d	coefficient of drag (1.95)
C_l	coefficient of lift (0.178)
f_s	coefficient of static friction (0.7)
g	acceleration of gravity (9.81 m/s^2)
θ	slope angle of beach (degrees)
$\rangle_b$	density of clast (1.8 t/m^3 for coral limestone)
$\rangle_w$	density of sea water (1.025 g/ml)
C_ρ	mixed-fluid density coefficient for seawater containing suspended sediments (1.087)[2]

[2] C_ρ is a multiplier for clear-seawater density, for conditions of elevated sediment content (as suspension and saltation load) during a tsunami. Here we adopt a conservative value of 5 % sediment concentration of basaltic (volcanic) sands and pebbles in the tsunami flow. See Terry and Malik (2020) for further details.

the field (Okal and Herbert, 2007, Moreno et al. 2009, supplementary fig. s2). Considering this, a local or regional tsunami, likely generated by a submarine landslide, seems the most likely explanation for a wave of sufficient magnitude.

To investigate the conjecture that a nearby submarine landslide could have created a localized tsunami that was responsible for transport of the clasts, a hypothetical source was created and the GeoClaw software was used to model the resulting tsunami and its impact on the Pūpuka pond region. For simplicity, we have assumed the landslide had the form of a submarine slump that can be modeled as a dipole source in which part of the seafloor drops while the neighboring seafloor rises (Fig. 5e). Similar sources have been used, for example, in modeling the submarine slump that probably accompanied the 1946 earthquake in the Aleutian Islands and the slump that created a large localized tsunami in Papua New Guinea in 1998 (Okal and Herbert, 2007; Watts et al., 2005; Fryer et al., 2004; Synolakis et al., 2002). The present-data bathymetry was modified by adding a function of the form:

$$\mathrm{D(x,y,t)} = \mathrm{A}\, sin(\pi\, \mathrm{x/L})\, sech^2(2.5 \times /\mathrm{L})\, sech^2(3\mathrm{y/W})\, \left(cos(\pi\, \mathrm{t/T}) + 1/2\right.$$

(for $|\mathrm{x}| < \mathrm{L}$, $0 \le \mathrm{t} \le \mathrm{T}$). In this formula, x and y are measured in meters. This source function is then placed at the desired location offshore and converted to UTM coordinates (longitude-latitude), after also rotating so that the main axis points in the desired direction. At the initial time $t = 0$ of the simulation this gives an additional mass on the seafloor that is uphill from a trough of equal volume. Over the specified time period of T seconds, the function D(x,y,t) decays toward the zero function, so that the present day bathymetry is recovered at later times. The length L, width W, and amplitude A can be adjusted to give a slump of any size. The maximum amplitude of the hump and trough are approximately equal to A, and the resulting tsunami has a similar peak amplitude.

As evidence that such a slump could produce a localized tsunami of the desired magnitude, we chose to center this source at 20.59 N, 156.2 W, which is on a relatively steep offshore slope roughly 4.5 km offshore from Nu'u, with an orientation that directs the largest waves toward the refuge. Currently there is no direct evidence of a submarine mass failure in this specific location, but bathymetry data indicate nearby landslide scarps (Fig. 5a). For hypothetical tsunami sources we fixed the slump dimensions with L = W = 3 km, and varied only the amplitude by setting A = 5, 10, or 15 m. The slumps modeled are thus similar in dimensions to the PNG 1998 model used by Watts et al. (2005) and plausible for a local slump event. We also used a similar time scale for motion, setting $T = 30$ s for all cases. Okal and Herbert (2007) used a similar shape but with larger dimensions for the landslide associated with the 1946 earthquake. Fig. 5a shows contours of the initial slump dipole and its location relative to Nu'u, along with a hillshade and pseudocolor representation of the bathymetry/topography.

More recent modeling of the PNG 1998 event and other landslide-generated tsunamis have used more sophisticated models of the landslide itself. But given the current lack of knowledge of the possible slump location and characteristics, in this work we simply illustrate that such an event could have created the deposits we study, and for this the simple source model adopted is sufficient. We note that a tsunami affecting Nu'u could also have come from a larger slump that was farther away, e.g. on the steeper slopes that are farther out in the 'Alenuihāhā channel. Such an event might still have been sufficiently localized that it was not observed or recorded elsewhere.

The time-dependent seafloor deformation described above was used as input to the open source software GeoClaw, which is distributed as part of Clawpack (Clawpack Development Team, 2024). This software solves two-dimensional depth-averaged fluid dynamics equations to model tsunami generation, propagation, and onshore inundation (Berger et al., 2011). We used version 5.10.0 of the software, which includes not only the nonlinear shallow water equations, which are often used for tsunami modeling, but also an implementation of dispersive Boussinesq-type equations that are better able to model

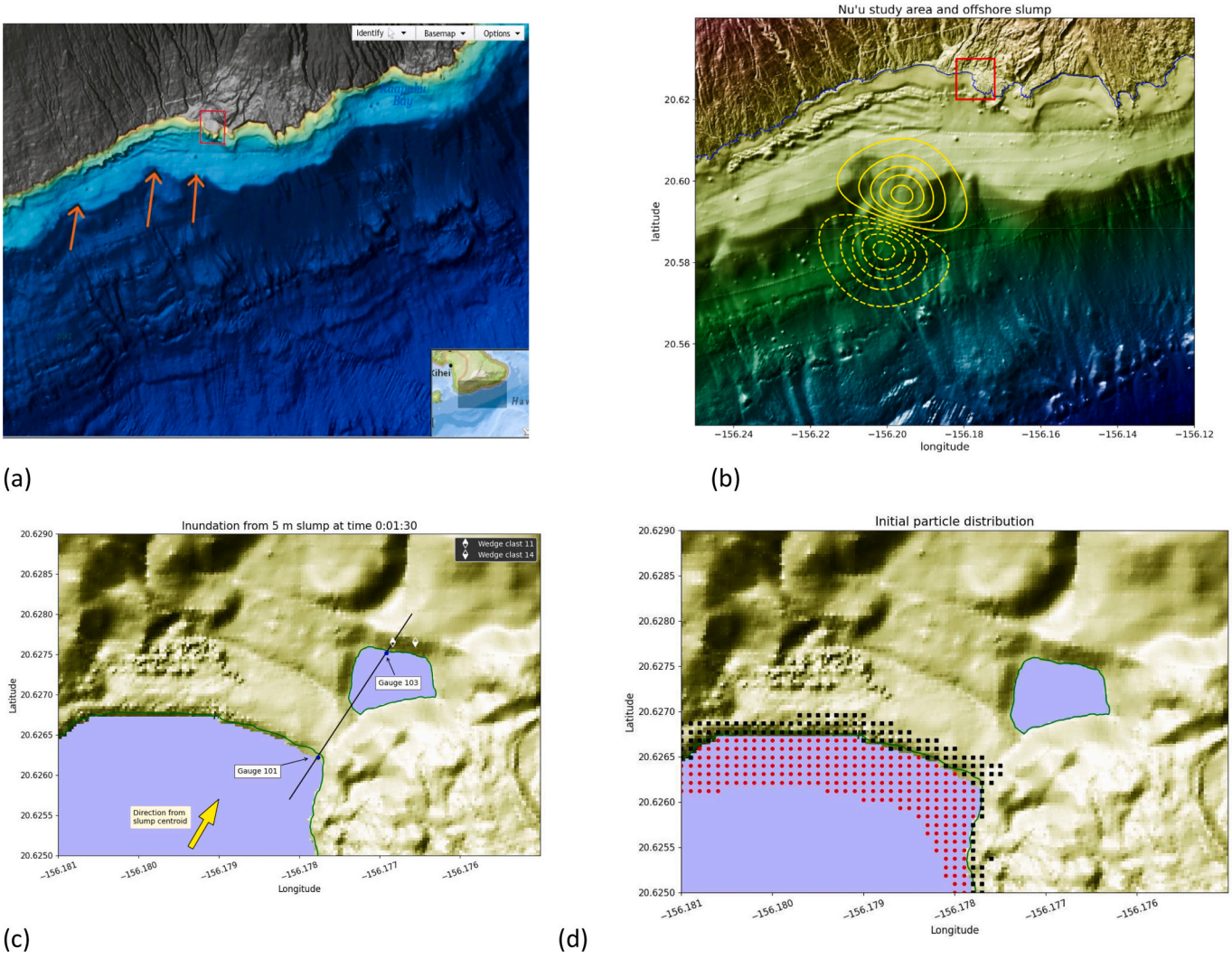

Fig. 5. (a) Slump dipole of modeled event; (b) gauge locations in Pūpuka pond, note the location of wedge clasts #11 and #14; (c) initial conditions of Nuʻu at the beginning of the modeled event; red circles depict source location of marine debris; black squares depict onshore basalt cobbles and boulders. (For interpretation of the references to colour in this figure legend, the reader is referred to the web version of this article.)

shorter wavelength tsunamis, such as those arising from localized slump events. The form of Boussinesq equations we used for this work are the modified Serre-Green-Naghdi equations proposed by Bonneton et al. (2011).

The present-day topography and bathymetry were used in this modeling, obtained from 6 arcsecond and 1/9 arcsecond DEMs distributed by NCEI (CUDEM 2024). The topography of the beach around Nuʻu was known to have been somewhat different in the past, based on historical maps (beach material has accreted recently), but for the hypothetical sources used here with adjustable amplitude, we believe the basic fluid dynamics around the Pūpuka pond region would have been similar. Animations of this event are included in the supplemental information.

4. Results

4.1. Accounts of high energy marine inundation (HEMI) events

Moʻolelo (orally transmitted accounts) of high energy marine inundation (HEMI) events are well known in Hawaiʻi (Brown, 2022; Beckwith, 1982; Maunupau, 1998). Such legends often encapsulate important traditional ecological knowledge as culturally encoded information associated with catastrophic events (Goff, 2023; Lauer and Matera, 2016).

Researchers have recorded a number of *moʻolelo* which describe catastrophic marine inundations across the archipelago, which have proven particularly useful to characterize the impacts of tsunamis on human communities (Brown, 2022; Beckwith, 1982; Anon, 1868; Anon., 1869). One particular legend from this area along Maui's south east coast (Fig. 1) describes the destruction of a fishpond by the Hawaiian deities Kāne and Kanaloa, the gods of agriculture and the ocean, respectively. As Maunupau (1998) describes it:

> *"A man who lived at Kahikinui [approximately 2.5 km from Nuʻu] had a fishpond that was famous for its fat fish. Kānemalaho was the name of this fishpond. One day two strangers came to the house of the native of Kahikinui. These were the gods Kāne and Kanaloa…When these strangers came the husband had gone fishing and only the wife was at home. They asked her for fish and she told them to wait until her husband came back, then they would have some fish. They were very angry with this answer, so they left to go to the fishpond where they broke it to pieces with their supernatural mana [spiritual power]. Then they went on their way to Nuʻu and Kaupō."*

Fishponds (*loko iʻa*) are common features of coastal ecosystems in Hawaiʻi, with over 350 *loko iʻa* of various types recorded on all of the main Hawaiian Islands (Keala, 2007). While *loko iʻa* frequently extend

from the shoreline into the ocean on shallow reef flats (creating a type known as a *loko kua pā*), in areas where off-shore water depth precludes such construction, fishponds were typically built inland from the coast, often near springs, in a type known as a *loko puʻuone* (Keala, 2007; Costa-Pierce, 1987). Considering the coastal bathymetry of the Kahikinui coast, Kanemalaho fishpond would have been a *loko puʻone,* constructed inland from the coast, likely in a natural spring-fed depression. Typically, the construction of fishponds did not involve dredging..

Although nothing in the telling of this *moʻolelo* specifically identifies this event as a tsunami, Kanaloa's supernatural powers associated with the ocean, would have likely been tacitly understood by the audience as a tsunami. Additionally, the presumed location of the fishpond inland from the coast argues against the likelihood of storm-driven waves, as these waves typically lose their energy only a short distance from the coast (Dewey et al., 2021; Goff et al., 2009). Tsunamis, however, with their wave energy throughout the entire wave column are known to cause substantial destruction far inland from the coast.

Maunupau's (1998) version of this legend contains only sparse details to constrain the chronology. However, the presence of a family who had constructed a fishpond, presumes permanent habitation. Archaeological work in both Kaupō and Kahikinui indicate settlement from the 15th-century onwards, constraining the date of this event to sometime afterwards (Baer, 2015; Kirch, 2014). More recent constraints of this event are also speculative, but stories involving traditional Hawaiian deities suggest a time prior to the arrival of Europeans in 1778 CE. In the original Hawaiian language version of this story, Maunupau (1998) suggests two words indicating the complete destruction of the fishpond, *wāwahi* (to dash to pieces) and *nāhāhā (*to break in pieces) (Pukui and Elbert, 1971). The use of these particular terms suggest the intensity of the destruction of the fishpond by these deities.

4.2. Wrack line distribution and chronological control

Wrack lines, or debris lines, of shells, coral and other off-shore material provide evidence of HEMI events, although in many cases distinguishing between storm surges and tsunamis can prove challenging (Richmond et al., 2011; Dodson et al., 2014). Distances from the coast provide the most useful diagnostic tool to distinguish between them, as tsunamis typically travel significantly further inland (Griswold et al., 2018; Watanabe et al., 2018).

Five coral clasts were collected from the wrack line on Kalaeʻapole which forms the approximate inland and upland extent of tsunami inundation (Fig. 2). The coral clasts ranged in size from 2.1 to 5.2 cm long and were collected for dating from elevations ranging from 6 to 8.5 m above msl (coral clasts 3 and 1, respectively). Inland distances ranged from 66.7 to 251 m from the coast (coral clasts 4 and 3, respectively; sup. Table s1). These dates range from 1671 CE to 878 CE (sup. Table s1). It is likely that the most recent date of 1671 CE corresponds to the maximum age of the tsunami which also imbricated the wedge clasts and transported the coral boulders inland to their current location. The three other coral clasts, which date to 1446 CE, 1274 CE, and 1071 CE, were likely reworked during the event (sup. Table s1).

The wide range of dates seen from the Nuʻu samples has a corollary with reported dates of depositional material from coastal ecosystems elsewhere. For example, Cundy et al. (2010) reported dates ranging nearly 2000 years from a coastal site in Greece. Ishizawa et al. (2020) also note the inherent challenge of dating tsunami deposits, pointing out that during wave run-up erosional processes tend to incorporate previously deposited material into the sedimentary mix. The range of dates found in the wrack line deposits likely reflect this process of reworking. However, it should be noted that the possibility of anthropogenic transportation, while unlikely, cannot be entirely ruled out.

4.3. Paleostage indicators (PSI)

A survey along a 1.25 km stretch of Nuʻu's coastal escarpment revealed a total of 16 vertical fractures containing a total of 37 wedge clasts. These included 34 waterworn basalt clasts and 3 coral fragments. Considering the large number of fractures along this portion of the coastal escarpment, ($n = 130$), wedge clasts were relatively uncommon.

Distances from the ocean ranged from 40 to 193 m, with the elevation of the highest clast, number 14, recorded at 8 m above msl (sup. Table s2). Measurements of accessible cobbles averaged 8.3 cm on the x-axis, 4.4 cm on the y-axis and 6.3 cm on the z-axis (sup. Table s2; note the inaccessibility of several cobbles). Considering the height of deposition and the size of the cobbles, bed load or saltation seems the most likely transport mechanism. We presume that the wave which transported these waterworn cobbles was the same as that which transported the coral boulders and the coral clasts found on Kalaeʻapole, although this cannot be conclusively proven.

4.4. Boulder deposits and flow velocity

Size data on 63 coral boulders were recorded, distributed between the northwest and southeast sides of Pūpuka pond (Fig. 2, sup. Fig. s1, sup. Table s3). The largest measured clast had a volume and mass of 0.054 m^3 and 28.1 kg respectively (clast ID #6 at Nu'u east; sup. Table s3). Using the system of Blott and Pye (2008) to define three-dimensional form of sedimentary particles, Nu'u coral clasts fall across various different categories (sup. Fig. s3), generally with blocky shapes (flat block – sub-equant block – elongate block). Nu'u southeast shows a higher proportion of blade and rod shaped clasts compared to Nu'u northwest, where these shapes are notably absent. Most of these boulders were scattered on the surface, although coral boulder #23 was embedded into the underlying substrate of Kalaeʻapole to a depth exceeding 20 cm, suggesting substantial flow velocity (sup.table s3).

Published hydrodynamic flow-transport (HFT) equations were used to calculate the minimum flow velocities (MFVs) necessary to initiate movement of coral clasts deposited at the study site. Calculated MFVs (Fig. 4) therefore provide a surrogate estimation of past tsunami magnitudes responsible for clast transport. All reef-derived coral clasts at Nu'u are assumed to have been either overturned (or lifted) during hydrodynamic transport from their original reef-platform (or reef-edge) sources. According to calculations, a 1.7 m/s MFV is required to set in motion the largest measured clast by overturning (rolling), with a higher 5.5 m/s MFV needed for clast lifting (saltation).

Note that if the HFT equations are based on clear seawater density (a common approach), without applying the mixed-fluid density coefficient (preferred here to represent more realistic elevated sediment concentrations (5 %) within the tsunami runup), then calculated MFV values are approximately 11 % higher (i.e. 1.8 m/s for overturning and 6.1 m/s for lifting the heaviest clast). In comparison, from field measurements of much larger transported carbonate reef blocks elsewhere in the Pacific Islands, (paleo)tsunami-induced nearshore MFVs have been estimated at 4.7 m/s (overturning) and 9.3 m/s (lifting) in Fiji and 7.3 m/s (overturning) and 16.3 m/s (lifting) in Kiribati (Terry et al., 2021, Lau et al., 2018). In both of these examples, localized tsunamis were probably caused by offshore submarine landslides, similar to the event suggested at Nu'u.

4.5. Modeling tsunami impacts

Submarine landslides are known to generate tsunamis around the Hawaiian Islands. These include an 1868 CE tsunami in the Kaʻū district of Hawaiʻi Island, the deadliest 19th century tsunami in the archipelago, as well as the most recent deadly tsunami in 1975 (Goff et al., 2006). As discussed below, Nuʻu experienced a destructive local tsunami in July of 1891 CE, likely derived from a submarine landslide in the ʻAlenuihāhā channel. While a Hawaiian language newspaper described this event, it is otherwise not widely known (Kalaowali, 1891). The fact that Nu'u previously experienced a local, presumably tsunamigenic submarine landslide raises the possibility that it had occurred before, and the

resident community captured this event in a *mo'olelo* passed down through the generations.

Models based on the two largest tsunamis to hit the Hawaiian Islands in the 20th century, the 1946 Aleutian Islands and the 1960 Valdivia Chile tsunamis, were created to evaluate their impacts at Nu'u, and to gauge if they had sufficient force to transport the materials evaluated in this study. These models demonstrated insufficient energy to transport either the wedge clasts or the coral boulders to their current locations (sup. Fig. S3). For this reason, this study used a hypothetical tsunami from a local source nearer the Nu'u Refuge. The local tsunami described above lends support to this assumption.

The random distribution of the coral boulders likely reflects tsunami-event (run-up and backwash) patterns of accumulation of coral and basalt material. Figs. 5–7 below illustrate the GeoClaw results for the three hypothetical events with wave amplitudes at the coast of A = 5, 10, and 15 m. Fig. 5a and b show the location of the tsunamigenic submarine landslide and two synthetic gauges where time series of water depth and speed were monitored during each simulation. Gauge 101 lies on the beach and Gauge 103 lies near the shore of the pond closest to a paleostage indicator found wedged above Pūpuka pond at an elevation of 3.2 m above msl (wedge clast #11 in sup. Table 1). Both gauges lie on a transect shown as a black line. Fig. 6 illustrates a time series of the gauge conditions with the various wave amplitudes in relation to these wedge clasts found above Pūpuka pond. The supplement includes animations of the tsunami amplitude on this transect over time.

In order to investigate the potential for the tsunami to bring clasts into the pond region from the beach, we used the fluid velocities calculated by GeoClaw to perform particle tracking, using the initial distribution of particles shown in Fig. 5c (Clawpack Development Team, 2024). Red circles represent hypothetical particles located offshore while black squares represent onshore particles, all in regions where the topography was within a few meters of sea level. Whereas we used a uniform initial distribution of particles, field observations at Nu'u suggest that long-shore drift causes accumulation of material to the east, next to Kalae'apole, likely influencing the difference between the modeled and actual distribution of the coral boulders.

The particle tracking was performed using a simplified model in which each particle moves with the local fluid velocity, but only when the fluid speed is greater than 5 m/s and the fluid depth is greater than 10 cm. Otherwise it is stationary. This determination is made every 2 s based on fluid velocities computed in the tsunami simulation, and moving particles are advanced by a simple forward Euler time step of 2 s (i.e., the displacement over this time step is the vector velocity in m/s multiplied by 2 s). There is no feedback from the particle motion to the fluid dynamics. It would be possible to include more complex particle dynamics, such as incorporating the mass of the particles along with static and dynamic friction forces if the particles are being dragged on the bottom. However, the clasts studied in this paper are small relative to the inundation depths, and we believe that this simple model of mobilization gives a sufficiently realistic indication of their possible motion and final resting place to illustrate the potential for a localized tsunami source to have created the observed depositional pattern.

Figure 7a, b and c show the location of these particles at time 3:30 min following initiation of the submarine slumps for the three cases studied (A = 5, 10, 15 m). This is roughly the time when the tsunami has reached its point of maximum inundation in each case. Similarly, Figs. 7d, e and f show the final distribution of particles after 20 min of simulated time for the three cases. A comparison of the modeled inundation generated by the 10 m slump shown in Fig. 7e with Fig. 2 shows the greatest degree of conformity between the modeled event and the actual deposition of both the paleostage indicators and coral boulders surrounding Pūpuka pond. Additionally, the elevation of the wedge clast above Pūpuka pond conforms to the modeled run up height at gauge 103 in Fig. 6b. This modeling suggests that a slump of approximately 10 m in this hypothetical location could have generated a wave (or sequence of waves) with a run up height reaching 8 m, which transported wedge

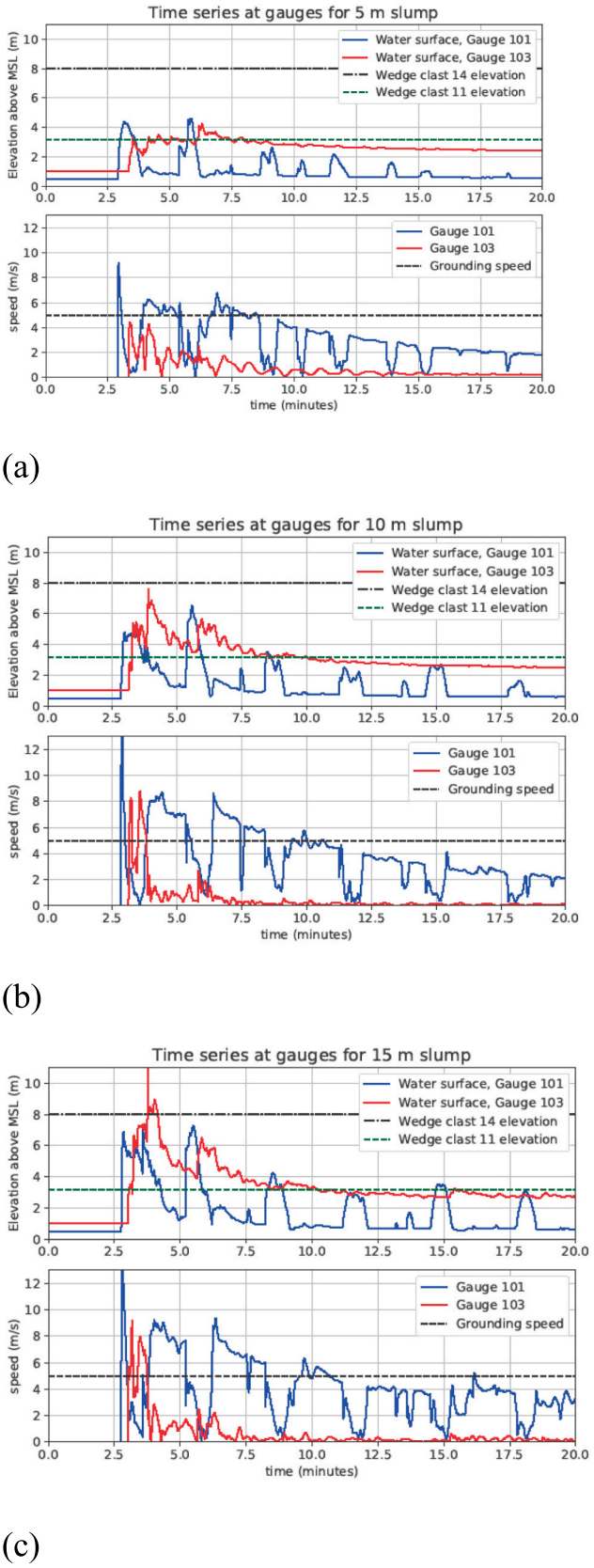

Fig. 6. Time series of gauge conditions at Pūpuka pond with wave amplitudes of (a) 5 m; (b)10 m; (c) 15 m.

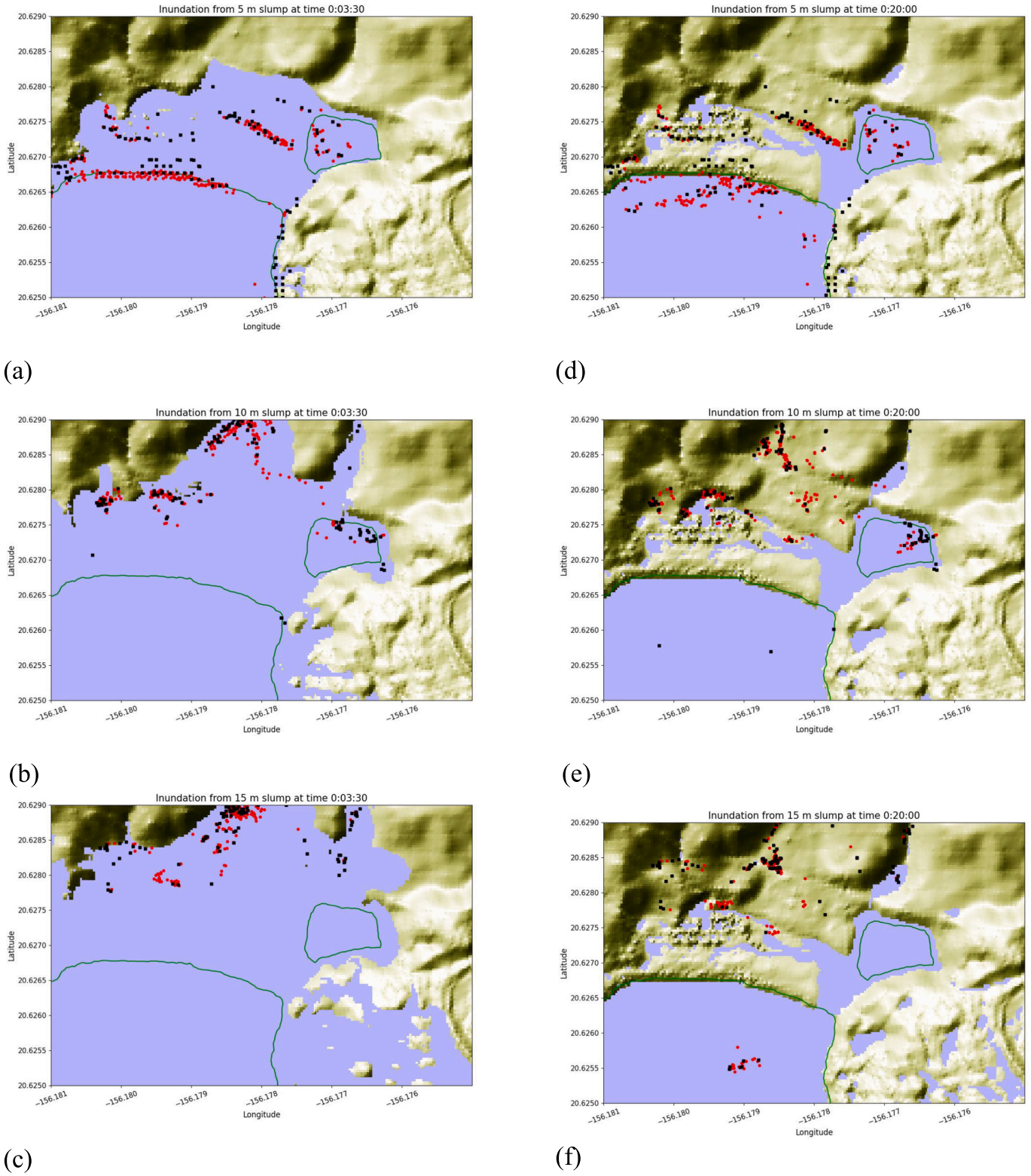

Fig. 7. Tsunami inundation at $t = 3{:}30$, as wave inundation is reaching its maximum with modeled slumps generating waves with amplitudes at the coast of (a) 5 m; (b) 10 m; (c) and 15 m and Tsunami inundation at $t = 20{:}00$, with wave amplitudes at the coast of (d) 5 m; (e) 10 m; and (f) 15 m. Red dots indicate coral boulders, while black dots indicate basalt boulders. (For interpretation of the references to colour in this figure legend, the reader is referred to the web version of this article.)

clasts at least 188 m inland (sup. Fig. s1). However, the deposition of the small coral clasts 251 m inland on Kalaeʻapole suggest the 15 m wave amplitude model may be a better fit.

5. Discussion

The *moʻolelo* (legend) of Kāne and Kanaloa destroying a fishpond along Maui's south east coast describes a destructive wave which could have impacted the Kaupō coast sometime after the 15th century, when

people permanently inhabited this area. While the legend does not contain a direct reference to a tsunami damaging the Pūpuka pond, its instigation by Kanaloa, the deity associated with the ocean, suggests a HEMI event (Beckwith, 1982). Data collected from the Nuʻu refuge support this *moʻolelo* as the result of a powerful tsunami in the pre-historic period. Coral boulders from the northwestern and south-eastern periphery of Pūpuka pond, paleostage indicators in the form of wedge clasts, and small coral clasts from Kalaeʻapole all point to an event larger than any known historical event (Fig. 2).

Moʻolelo of suspected local tsunamis are documented at other locations across the Hawaiian Islands. For example, a chant composed in the 16th century by Huluamana, a resident of Kalaeloa, on the east central coast of Molokaʻi records a wave which killed the residents of this village (Fig. 1, Lander and Lockridge, 1989). While we cannot discount the possibility that this wave and the one at Nuʻu describe the same event, so far no records have emerged of similar inundations affecting other areas of south Mauiʻs densely populated coast, particularly the village of Lāhaina (Fig. 1).

Minimum flow velocities indicate speeds up to 1.6–5.5 m/s, while wave runup heights estimated from wedge-clast paleostage indicators suggest run up heights around 8 m above msl (Figs. 2 and 4, sup. Table s2). Small coral clasts from Kalaeʻapole provide a chronological control for the tsunami which deposited them and indicate an event date around the late 17th to late 18th century. These small coral clasts also suggest wave runup heights between 8 and 8.5 m and inland inundation distances up to 251 m (sup. Table s1). Modeling of this event, which takes into account the proxies discussed above, suggest a local, rather than regional or distant-source, tsunami (Fig. 7). This model of material deposited during a tsunamigenic submarine landslide off the coast of Nuʻu substantially conformed to the data collected from the coral boulders, paleostage indicators and small coral clasts used in this study (Figs. 2 and 7). Considering this, it seems plausible that an offshore submarine landslide triggered this event, possibly originating from the steep slopes of the ʻAlenuihāhā channel.

Terry et al. (2019), Goff and Terry (2016) and Goff (2011) note that oceanic volcanoes, which includes Haleakalā, are subject to submarine slope failure. While subduction zone earthquakes generate the majority of recorded trans-Pacific tsunamis, sub-aerial and submarine landslides are responsible for at least 10 % of recorded tsunamis worldwide, if not considerably more (Goff, 2011; Goff and Cain, 2016). Historical records have implicated a submarine landslide (also known as a submarine mass failure) in the South China Sea for the death of 40,000 people around Taiwan in 1781 CE or 1782 CE (Dodson et al., 2014). One of the most destructive 20th century tsunamis occurred on July 17, 1998 when an earthquake and submarine landslide offshore of ʻAitape, Papua New Guinea generated a tsunami with wave heights exceeding 15 m (Dawson and Stewart, 2007b; McSaveney et al., 2000). This tsunami killed at least 2200 individuals, with inland inundation distances exceeding 400 m (Jaffe et al., 2008; Okal and Herbert, 2007).

In the Hawaiian islands, sedimentary debris from Pleistocene submarine landslide generated tsunamis has been documented on the islands of Hawaiʻi, Molokaʻi and Lānaʻi (Fig. 1, Moore, 2008, Webster et al., 2006, McMurtry et al., 2004; Johnson and Mader, 1995; Moore et al., 1994; Moore and Moore, 1988; Moore and Moore, 1984). Researchers have noted two sources for submarine landslides, known as Alika I and II, originating from the southwestern flank of Hawaiʻi Island. Alika I occurred sometime between 240 and 200 ka BP, with runup heights recorded between 46 and 60 m. Evidence for the Alika II submarine landslide dates to between 120 and 105 ka BP, with measured runup elevations on the island of Lānaʻi of 375 m (McMurtry et al., 2004, Johnson and Mader, 1995, Moore et al., 1994, Moore and Moore, 1988, Moore and Moore, 1984). However, other researchers have questioned the validity of the claims for tsunami deposition, noting that lithospheric flexure offers an equally plausible scenario (Keating and Helsley, 2012; Rubin et al., 2000; Grigg and Jones, 1997).

Notwithstanding this debate, four known historic tsunamigenic submarine landslides were recorded in the Hawaiian Islands in the 19th and 20th centuries. The first of these took place in the Halapē-ʻĀpua area of Hawaiʻi Island after a Mw 7.5 earthquake occurred on April 3rd, 1868 CE (Fig. 1, Goff et al., 2006). This event killed 47 individuals and destroyed 108 homes in the village of ʻĀpua, leading to its abandonment. A survey in the aftermath of this event noted that waves estimated at 6 m had "swept over the top of the cocoanut [sic] trees" (Anon, 1868). A year later, on the 24th of July 1869 CE a tsunami flooded villages along the Puna coast of Hawaiʻi Island, several kilometers north of the previous year's event, with inundation distances reported up to 270 m with water overtopping a 4.5 m embankment (Fig. 1, Anon., 1869).

A third event, likely from a submarine landslide in the ʻAlenuihāhā channel, damaged homes and covered the Pili o Kāne spring on the northern edge of Nuʻu's Pūpuka pond (Fig. 2) on the 18th of July 1891 CE (Kalaowali, 1891). Local residents reported inundation distances of approximately 150 m inland. Reports of this event were limited to Nuʻu, suggesting a local event, although relatively little is known of this incident beyond one reference in the Hawaiian language newspaper *Ka Leo o ka Lāhui*.

Hawaiʻi's most recent deadly tsunami, also a local event, struck Hawaiʻi Island in the area of Halapē-ʻĀpua (in the same vicinity as the April 1868 CE event) when a tsunamigenic submarine landslide occurred in the early morning hours of November 29th, 1975, killing two and injuring 19 campers (Goff et al., 2006). A survey which followed this event estimated wave heights of 5 m with inundation distances of 250 m (Lander and Lockridge, 1989). These historically recorded events demonstrate that locally generated tsunamis can produce wave heights of 6 m or greater and inundation distances of nearly 300 m are possible and can occur along the same coastline. As the data and modeling here suggest, locally-generated tsunamis from submarine landslides warrant further attention and research in the Hawaiian Islands as sources of destructive HEMI events.

6. Conclusion

We hypothesized that a legend passed down through the generations describes a local, pre-historic tsunami from Maui's south east coast. As the agent of this event, Kanaloa, the deity associated with the ocean, suggests a tsunami as the culprit. Field investigations at Nuʻu along Maui's south east coast suggest the veracity of this *moʻolelo*. This legend suggests the importance of indigenous knowledge as an avenue for future paleotsunami research.

Data gathered from small coral clasts, wedge clasts and coral boulders provide critical evidence of the destructive power of this tsunami and support this hypothesis. The data suggests this event took place sometime between 1671 CE and 1778 CE, and witnessed runup heights of at least 8 m with inundation distances of at least 200 m, and minimum flow velocities reaching 5 m/s. The power of this wave, as demonstrated by the inland deposition of the coral boulders in particular, suggests a tsunami rather than a large storm. Additionally, the lack of recorded trans-Pacific tsunamis capable of the degree of inundation witnessed from this event suggests the likelihood of a local tsunami.

Particle deposition from a hypothetical slump-generated tsunami occurring in the ʻAlenuihāhā channel near the Nuʻu Refuge shows broadly similar patterns to data gathered from field investigations. A review of historically documented local tsunamis, including a smaller event generated offshore of Nuʻu in July 1891 CE, suggests the plausibility of a local tsunami generated in the ʻĀlenuihāhā channel. This research demonstrates the importance of research on locally-generated tsunamigenic submarine landslides, while the efficacy of this approach rests on understanding both the cultural expressions of these events as well as their source mechanisms.

Supplementary data to this article can be found online at https://doi.org/10.1016/j.margeo.2024.107408.

Data availability and additional information

The tsunami simulations described in the supplementary section of the paper were performed using GeoClaw from version 5.10.0 of the open source Clawpack software, freely available from [www.clawpack.org] and published with a nonrestrictive BSD software license. The custom code that was used to drive the simulations and produce the graphics presented in this paper, and the Jupyter notebook and animations available in the SI, is available in the Github repository https://github.com/rjleveque/NuuRefugeTsunami. Upon publication of this paper, a permanent snapshot of the final code used will be archived on Zenodo with a DOI inserted there.

CRediT authorship contribution statement

Scott Fisher: Writing – review & editing, Writing – original draft, Formal analysis, Data curation, Conceptualization. **James Goff:** Investigation, Data curation, Conceptualization. **Andrew Cundy:** Writing – review & editing, Supervision, Conceptualization. **David Sear:** Writing – review & editing, Supervision, Formal analysis, Data curation, Conceptualization. **James Terry:** Writing – review & editing, Formal analysis, Data curation, Conceptualization. **Randall J. LeVeque:** Writing – review & editing, Software, Methodology, Data curation, Conceptualization. **Loyce M. Adams:** Writing – review & editing, Software, Methodology, Data curation, Conceptualization. **Diana Sahy:** Data curation, Formal analysis.

Declaration of competing interest

The authors declare that they have no known competing financial interests or personal relationships that could have appeared to influence the work reported in this paper. JG is an Editor-in-Chief for Natural Hazards and was not involved in the editorial review or the decision to publish this article.

Acknowledgements

The authors wish to thank the three reviewers who provided helpful feedback on this manuscript. The authors also wish to thank Mr. David Lawrence, Mr. Robert Hobdy, Mr. Bill Levien and the high school students at Seabury Hall who assisted with some of the field investigations. Research on tsunami debris tracking was supported in part by the Cascadia CoPes Hub, NSF grant 203713.

References

Anon, 1868. Notes of the Week, Earthquakes and the Volcano. Pacific Commercial Advertiser, 619-6m.
Anon., 1869. Kū ke ʻa ka hale o Kaupō, Ka nupepa kuokoa, Augate 14, 1869. VIII: 33.
Baer, A., 2015. On the Cloak of Kings: Agriculture, Power, and Community in Kaupō, Maui. Ph.D. Dissertation. University of California Berkeley, Berkeley.
Beckwith, M., 1982. Hawaiian Mythology. University of Hawai'i Press, Honolulu.
Berger, M., George, D., LeVeque, R., Mandli, K., 2011. The GeoClaw software for depth-averaged flows with adaptive refinement. Adv. Water Resour. 34, 1195–1206.
Blott, S.J., Pye, K., 2008. Particle shape: a review and new methods of characterization and classification. Sedimentology 55, 31–63.
Bonneton, P., Chazel, F., Lannes, D., Marche, F., Tissier, M.A., 2011. Splitting approach for the fully nonlinear and weakly dispersive Green-Naghdi model. J. Comput. Phys. 230, 1479–1498.
Bosserelle, C., Williams S., Cheung, K.F., Lay T., Yamazak I Y., Simi T., Roeber V., Lane E., Paulik R., Simanu L., 2020 Effects of source faulting and fringing reefs on the 2009 South Pacific Tsunami Inundation in Southeast Upolu, Samoa. J. of Geog. Res.: Oceans, 125, 1–15.
Brown, M.A., 2022. Ka Poʻe Moʻo Akua: Hawaiian Reptilian Water Deities. University of Hawai'i Press, Mānoa.
Bruland, G.L., MacKenzie, R.A., 2010. Nitrogen source tracking with δ15N content of coastal wetland plants in Hawaii. J. Environ. Qual. 39, 409–419.
Cain, G., Goff, J., McFadgen, B., 2007. Prehistoric mass burials: did death come in waves? J. Archaeol. Method Theory 26, 719–754.
Clark, G., Reepmeyer, C., 2014. Stone architecture, monuments and the rise of the early Tongan chiefdom. Antiq 88, 1244–1260.
Clawpack Development Team, . Clawpack software. http://www.clawpack.org. https://doi.org/10.17605/osf.io/kmw6h.
Costa-Pierce, B.A., 1987. Aquaculture in Ancient Hawai'i. BioSci 37 (5), 320–331.
Crémière, A., Lapland, A., Chand, S., Sahy, D., Condon, D.J., Noble, S.R., Martma, T., Thorsnes, T., Sauer, S., Brunstad, S., 2016. Timescales of methane seepage on the Norwegian margin following collapse of the Scandinavian Ice Sheet. Nat. Commun. 7, 11509.
Cundy, A.B., Gaki-Papanastassiou, K., Papanastassiou, D., Maroukian, H., Frogley, M.R., Cane, T., 2010. Geological and geomorphological evidence of recent coastal uplift along a major Hellenic normal fault system (the Kamena Vourla fault zone, NW Evoikos Gulf, Greece). Mar. Geol. 271 (1–2), 156–164.
Dawson, A., Stewart, I., 2007a. Tsunami deposits in the geological record. Sediment. Geol. 200, 166–183.
Dawson, A., Stewart, I., 2007b. Tsunami geoscience. Prog. Phys. Geogr. 31, 575–590.
Dewey, J.F., Goff, J., Ryan, P.D., 2021. The origins of marine and non-marine boulder deposits: a brief review. Nat. Hazards 109, 1981–2002. https://doi.org/10.1007/s11069-021-04906-3.
Dodson, J., Eliot, I., Eliot, M., Chagué-Goff, C., Goff, J., 2014. Wrack line signatures of high-magnitude water-level events on the northwest Australian coast. Mar. Geol. 355, 310–317.
Etienne, S., Buckley, M., Paris, R., Nandasena, A.K., Clark, K., Strotz, L., Chagué-Goff, C., Goff, J., Richmond, B., 2011. The use of boulders for characterising past tsunamis: lessons from the 2004 Indian Ocean and 2009 South Pacific tsunamis. Earth Sci. Rev. 107, 76–90.
Fisher, S., Goff, J., Cundy, A., Sear, D., 2023. A qualitative review of tsunamis in Hawai'i. Nat. Hazards 118, 1797–1832.
Frohlich, C., Hornbach, M.J., Taylor, F.W., Shen, C.C., Moala, A., Morton, A., Kruger, J., 2009. Huge erratic boulders in Tonga deposited by a prehistoric tsunami. Geol 37, 131–134.
Fryer, G.J., Watts, P., Pratson, L.F., 2004. Source of the great tsunami of 1 April 1946: a landslide in the upper Aleutian forearc. Mar. Geol. 203, 201–218.
Goff, J., 2011. Evidence of a previously unrecorded local tsunami, 13 April 2010, Cook Islands: implications for Pacific Island Countries. Nat. Hazards Earth Syst. Sci. 11, 1371–1379.
Goff, J., 2023. In Search of Ancient Tsunamis: A Researcher's Travels, Tools, and Techniques. Oxford University Press, London.
Goff, J., Cain, G., 2016. Tsunami databases: the problems of acceptance and absence. Geoforum 76, 114–117. https://doi.org/10.1016/j.geoforum.2016.09.005.
Goff, J., Dudley, W., 2021. Tsunami: The World's Greatest Waves. Oxford University Press, New York.
Goff, J., Nunn, P.D., 2016. Rapid societal change as a proxy for regional environmental forcing: evidence and explanations for Pacific Island societies in the 14–15th centuries. Isl Arch. 25, 305–316.
Goff, J., Terry, J., 2016. Tsunamigenic slope failures: the Pacific Islands 'blind spot'? Landslides 11, 1535–1543.
Goff, J., Dudley, W.C., deMaintenon, M.J., Cain, G., Coney, J.P., 2006. The largest local tsunami in 20th century, Hawaii. Mar. Geol. 226, 65–79.
Goff, J.R., Chagué-Goff, C., 2009. Brief communications: cetaceans and tsunamis-whatever remains, however improbably, must be the truth? Nat. Hazards Earth Syst. Sci. 9, 855–857.
Goff, J.R., McFadgen, B.G., 2001. Catastrophic seismic-related events and their impact on prehistoric human occupation, coastal New Zealand. Antiquity 75, 155–162.
Goff, J.R., Lane, E., Arnold, J., 2009. The Tsunami geomorphology of coastal dunes. Nat. Hazards Earth Syst. Sci. 9, 847–854.
Goto, K., Miyagi, K., Kawamata, H., Imamura, F., 2010. Discrimination of boulders deposited by tsunamis and storm waves at Ishigaki Island, Japan. Mar. Geol. 269, 34–45.
Gregg, T.M., Mead, L., Burns, J.H.R., Takabayashi, M., 2015. Puka Mai he Koʻa: The significance of Corals in Hawaiian Culture. In: Narchi, N., Price, L. (Eds.), Ethnobiology of Corals and Coral Reefs. Springer, pp. 103–115.
Grigg, R.W., Jones, A.T., 1997. Uplift caused by lithospheric flexure in the Hawaiian archipelago as revealed by elevated coral deposits. Mar. Geol. 141, 11–25.
Griswold, F.R., MacInnes, B.T., Higman, B., 2018. Tsunami-based evidence for large eastern Aleutian slip during the 1957 earthquake. Quat. Res. 91, 1–14.
Ishizawa, T., Goto, K., Yokoyama, Y., Goff, J., 2020. Dating tsunami deposits: present knowledge and challenges. Earth Sci. Rev. 200, 1–11.
Jaffe, B.E., Morton, R.A., Kortekaas, S., Dawson, A.G., Smith, D.E., Gelfenbaum, G., Foster, I.D.L., Long, D., Shi, S., 2008. Reply to Bridge (2008) discussion of articles in 'sedimentary features of tsunami deposits.'. Sediment. Geol. 211, 95–97.
Jarrett, R.D., England Jr., J.F., 2002. Reliability of paleostage indicators for paleoflood studies. In: House, P.K., Webb, R.H., Baker, V.R., Levish, D.R. (Eds.), Ancient Floods, Modern Hazards: Principles and Applications of Paleoflood Hydrology, Water Science and Application, vol. 5. Am. Geophys. Union, pp. 91–109.
Johnson, C., Mader, C.L., 1995. Modeling the 105 Ka Lanai Tsunami. Sci. Tsunami Haz. 12, 33–38.
Juvik, S., Juvik, J., 1999. Atlas of Hawai'i, 3rd edition. University of Hawai'i Press, Honolulu.
Kalaowali, W., 1891. Nā mea hou ma Nuʻu, Kaupō [Recent events at Nuʻu, Kaupō]. In: Ka Leo o Ka Lāhui [The voice of the Nation].
Keating, B., Whelan, F., Bailey-Brock, J., 2004. Tsunami deposits at Queen's Beach, Oahu, Hawaii-initial results and wave modeling. Sci. Tsunami Haz. 22, 23–43.
Keala, G., 2007. Loko iʻa: A Manual on Hawaiian Fishpond Restoration and Management. University of Hawai'i, Mānoa, College of Tropical Agriculture and Human Resources, Honolulu.
Keating, B.K., Helsley, C.E., 2012. Traces of coral bearing deposits on Lanai, Hawaii, and implications for their origin (island uplift versus giant tsunami). In: Lopez, G. (Ed.),

Tsunami-Analysis of a Hazard-from Physical Interpretation to Human Impact. Intech, pp. 225–258.
Kirch, P.V., 2014. Kuaʻāina Kahiko: Life and Land in Ancient Kahikinui, Maui. University of Hawaiʻi Press, Honolulu.
Kirch, P.V., Holson, J., Baer, A., 2009. Intensive dryland agriculture in Kaupō, Maui, Hawaiian Islands. Asian Perspect. 48, 265–290.
Lander, J.F., Lockridge, P.A., 1989. United States Tsunamis (Including United States Possessions) 1690–1988. National Geophysical Data Center, Boulder, Colorado.
Lau, A.Y.A., Terry, J.P., Ziegler, A., Pratap, A., Harris, D., 2018. Boulder emplacement and remobilisation by cyclone and submarine landslide tsunami waves near Suva City, Fiji. Sediment. Geol. 364, 242–257.
Lauer, M., Matera, J., 2016. Who detects ecological change after catastrophic events? Indigenous knowledge, social networks, and situated practices. Hum. Ecol. 44, 33–46.
Lavigne, F., Morin, J., Wassmer, P., Weller, O., Kula, T., Maea, A.V., Kelfoun, K., Mokadem, F., Paris, R., Malwani, M., Ngainui, F., Audrey, B.M., Saulnier-Copard, S., Vidal, C.M., Tuʻiʻahai, T., Kitekeiʻaho, F., Trautmann, M., Gomez, C., 2021. Bridging legends and science: feld evidence of a large tsunami that affected the Kingdom of Tonga in the 15th century. Front. Earth Sci. 9, 1–15.
Loomis, Harold G., 1976. Tsunami Wave Runup Heights in Hawaii. Hawaii Institute of Geophysics, Manoa.
Maunupau, T., 1998. Huakaʻi Makaʻikaʻi a Kaupō, Maui: A Visit to Kaupō, Maui. Hawaiian and English version. Trans. by Roger Rose and Noelanikoʻolau Losch. Honolulu Bishop Museum Press.
McClintock, J., Goff, J., McFadgen, B., 2023. Reconstructing a palaeotsunami: geomorphological and cultural change associated with a catastrophic 15th century event, Kāpiti Coast, Aotearoa/New Zealand. The Holocene 34, 1–10.
McMurtry, G.M., et al., 2004. Megatsunami deposits on Kohala Volcano, Hawaii, from flank collapse of Mauna Loa. Geol. Soc. Am. 32, 741–744.
McSaveney, M.J., Goff, J., Darby, D., Goldsmith, P., Barnett, A., Elliott, S., Nongkas, M., 2000. The 17 July 1998 tsunami, Papua New Guinea: evidence and initial interpretation. Mar. Geol. 170, 81–92.
Moore, A.L., 2008. Landward fining in onshore gravel as evidence for a late pleistocene tsunami on Molokai, Hawaii. Geol 28, 247–250.
Moore, G.W., Moore, J.G., 1988. Large scale bedforms in boulder gravel produced by giant waves in Hawaii. Geol. Soc. Am. Spec. Pap. 229, 101–110.
Moore, J.G., Moore, G.W., 1984. Deposit from a giant wave on the island of Lānaʻi, Hawaii. Sci 226, 1312–1315.
Moore, J.G., Bryan, W.B., Ludwig, K.R., 1994. Chaotic deposition by a giant wave, Molokai, Hawaii. Geol. Soc. Am. Bull. 106, 962–967.
Moreno, M.S., Bolte, J., Klotz, J., Melnick, D., 2009. Impact of megathrust geometry on inversion of coseismic slip from geodetic data: application to the 1960 Chile earthquake. Geophys. Res. Lett. 36, L16310.
Nandasena, J.A.K., Paris, R., Tanaka, N., 2011. Numerical assessment of boulder transport by the 2004 Indian ocean tsunami in Lhok Nga, West Banda Aceh (Sumatra, Indonesia). Comput. Geosci. 37, 1391–1399.
O`Connor, J.E., Baker, V.R., 1992. Magnitudes and implications of peak discharge from glacial Lake Missoula. Geol. Soc. Am. Bull. 104, 2667–279.
Okal, E.A., Herbert, H., 2007. Far-field simulation of the 1946 Aleutian tsunami. Geophys. J. Int. 169, 1229–1238.
Pukui, M.K., Elbert, S.H., 1971. Hawaiian Dictionary: Hawaiian-English, English-Hawaiian. University of Hawaiʻi Press, Honolulu.
Reid, J.A., Mooney, W.D., 2023. Tsunami Occurrence 1900–2020: a Global Review, with examples from Indonesia. Pure Appl. Geophys. 180, 1549–1571.
Richmond, B.M., Buckley, M., Etienne, S., Chagué-Goff, C., Clark, K., Goff, J., Dominey-Howes, D., Strotz, L., 2011. Deposits, flow characteristics, and landscape change resulting from the September 2009 South Pacific tsunami in the Samoan Islands. Earth Sci. Rev. 107, 38–51.
Rubin, K.H., Fletcher III, C.H., Sherman, C., 2000. Fossiliferous Lanaʻi deposits formed by multiple events rather than a single giant tsunami. Nat 407, 675–681.
Sherrod, D.R., Hagstrum, J.T., McGeehin, J.P., Champion, D.E., Trusdell, F.A., 2006. Distribution, 14C chronology, and paleomagnetism of latest pleistocene and holocene lava flows at Haleakalā volcano, island of Maui, Hawaiʻi: a revision of lava flow hazard zones. J. Geophys. Res. 111, 1–24.
Shtienberg, G., Yasur-Landau, A., Norris, R.D., Lazar, M., Rittenour, T.M., Tamberino, A., Gadal, O., Kantu, K., Arken-Shalev, E., Ward, S.N., Levey, T.E., 2020. A neolithic mega-tsunami event in the eastern Mediterranean: prehistoric settlement vulnerability along the Carmel coast, Israel. PLoS One 15, 1–15.
Smith, D.E., Shi, S., Cullingford, R.A., Dawson, A.B., Dawson, S., Firth, C.R., Foster, I.D. L., Fretwell, P.T., Haggart, B.A., Holloway, L.K., Long, D., 2004. The holocene Storegga slide tsunami in the United Kingdom. Quat. Sci. Rev. 23, 2291–2321.
Synolakis, C.E., Bardet, J.P., Borrero, J.C., Davies, H.L., Okal, E.A., Silver, E.A., Sweet, S., Tappin, D.R., 2002. The slump origin of the 1998 Papua New Guinea tsunami. Proc. Roy. Soc. Lond. Ser. A: Math. Phys. Eng. Sci. 458, 763–789.
Tanaka, N., Nandasena, N.A.K., Jinadasa, K.B.S.N., Sasaki, Y., Tanimoto, K., Mowjood, M.I.M., 2009. Developing effective vegetation bioshield for tsunami protection. Civ. Eng. Environ. Syst. 26, 163–180.
Terry, J.P., Malik, S.A., 2020. Reconsidering the seawater-density parameter in hydrodynamic flow transport equations for coastal boulders. New Zeal. J. Geol. Geophys. 63, 363–370.
Terry, J.P., Goff, J., Winspear, N., Bongolan, V.P., 2019. Recognising the perils of landslide-generated tsunamis in the Asia–Pacific region. Nat. Hazards 97, 1413–1416.
Terry, J.P., Karoro, R., Gienko, G.A., Wieczorek, M., Lau, A.Y.A., 2021. Giant palaeotsunami in Kiribati: converging evidence from geology and oral history. Island Arc 30, e12417. https://doi.org/10.1111/iar.12417.
Walmisley, A.J., 2021. The Betrayal of Elia Helekunihi: Hawaiian Patriot or Haole Pet? The Politics of Tradition and Colonisation by Stealth in 19th Century Hawaiʻi. Ph.D. thesis. University of Birmingham, Birmingham, UK.
Watanabe, M., Goto, K., Bricker, J.D., Imamura, F., 2018. Are inundation limit and maximum extent of sand useful for differentiating tsunamis and storms? An example from sediment transport simulations on the Sendai Plain, Japan. Sediment. Geol. 264, 204–216.
Watts, P., Grilli, S.T., Tappin, D.R., Fryer, G.J., 2005. Tsunami generation by submarine mass failure. II: predictive equations and case studies. J. Waterw. Port Coast. Ocean Eng. 131, 298–310.
Webster, J.M., Clague, D.A., Braga, J.C., 2006. Support for the giant wave hypothesis: evidence from submerged terraces of Lanai, Hawaii. Int. J. Earth Sci. 96, 517–524.